

Photochemical "Across-a-Ridge" *Z*–*E* Isomerization of (Ethenyl-2-*d*)anthracenes in the Triplet State

Takashi Karatsu,^{*,†,‡} Hiroaki Misawa,^{*,†,§} Mikiko Nojiri,[‡] Naoko Nakahigashi,[‡] Seiichi Watanabe,[†] Akihide Kitamura,[†] Tatsuo Arai,[‡] Hirochika Sakuragi,[‡] and Katsumi Tokumaru^{*,‡}

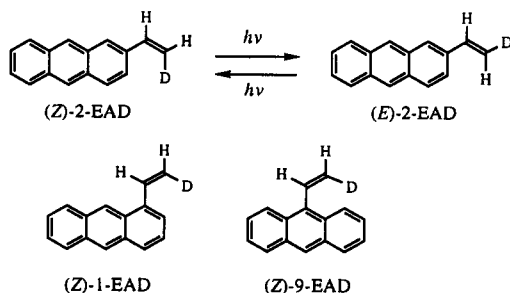
College of Arts and Sciences, Chiba University, 1-33 Yayoi-cho, Inage-ku Chiba 263, Japan, and Department of Chemistry, University of Tsukuba, Tsukuba, Ibaraki 305, Japan

Received: July 7, 1993; In Final Form: October 20, 1993*

Deuterated ethenylanthracenes, 1-, 2-, and 9-(ethenyl-(*Z*)-2-*d*)anthracene, and 2-(ethenyl-(*E*)-2-*d*)anthracene ((*Z*)-1-, 2-, and 9-EAD, and (*E*)-2-EAD, respectively) undergo photochemical *Z*–*E* isomerization under thermal activation. The temperature dependence of their isomerization quantum yields and the temperature independence of lifetimes of their $T_n \leftarrow T_1$ absorptions indicate that EADs isomerize adiabatically between the *Z* and *E* isomers in the lowest excited triplet state by overcoming an activation barrier ($E_a = 19$ – 46 kJ mol⁻¹) of the perpendicularly twisted geometry. The activation parameters of isomerization, ΔH^\ddagger (17–42 kJ mol⁻¹) and ΔS^\ddagger (–40 to –113 J K⁻¹ mol⁻¹), decrease in the order of 2-, 1-, and 9-isomers; however, ΔG^\ddagger (50–54 kJ mol⁻¹) is almost constant irrespective of the substitution position of the anthracene nucleus.

1. Introduction

It was well recognized that on triplet sensitization olefins such as styrenes^{1–3} and stilbenes^{4–10} undergo mutual isomerization between the *Z* and *E* isomers through a perpendicularly twisted geometry of the triplet state (³p*). On the other hand, we have recently found that anthrylethylenes like 2-(3,3-dimethyl-1-butenyl)anthracene (2-DMBA) undergo adiabatic one-way isomerization from *Z* triplets (³Z*) to *E* triplets (³E*) by passing over an energy barrier at ³p* without involving deactivation from ³p* to the ground-state twisted geometry.^{11–16} To get further insight into the potential energy surface of the triplet state, we worked with a deuterated derivative of 2-ethenylanthracene, 2-(ethenyl-(*E*)-2-*d*)anthracene ((*E*)-2-EAD), which possesses essentially symmetrical energy surfaces about rotation of the ethylenic bond in the ground and triplet states, and found that the isomerization of (*E*)-2-EAD proceeds at temperature higher than 17 °C with an activation energy of nearly 46 kJ mol⁻¹, which corresponds to the energy difference between ³E* and ³p*.¹⁷ We have extended the work to deuterated derivatives of the isomeric 1- and 9-ethenylanthracenes, 1-EAD and 9-EAD, together with further consideration of the results of 2-EAD, and now report electronic and steric effects of the substitution position of the ethenyl group on the isomerization and the potential energy surfaces.



2. Experimental Section

Materials. 1- and 2-ethenylanthracene (1- and 2-EA) were prepared according to the reference.¹⁸ 9-Ethenylanthracene (9-EA, Aldrich) was commercially obtained and crystallized from ethanol.

2-(Ethenyl-(*Z*)-2-*d*)anthracene. 2-Ethenylanthracene (9.0 g, 44 mmol) was allowed to react with bromine (7.1 g, 44 mmol) in carbon disulfide (200 mL) to give 2-(1,2-dibromoethyl)-anthracene (yield 14.0 g, 87%).

The dibromide (14.0 g, 38 mmol) was dehydrobrominated in THF (200 mL) with sodium amide¹⁹ prepared from liquid ammonia (300 mL) and sodium (7.0 g, 0.30 mol). Column chromatography (SiO₂, hexane) of the crude product afforded 2-ethynylanthracene (2.7 g, 35%); ¹H NMR (CDCl₃) δ 3.20 (s, 1H, C \equiv CH), 7.35–7.53 (m, 3H, ArH), 7.87–8.20 (m, 4H, ArH), 8.37 (s, 2H, ArH).

To a solution of 2-ethynylanthracene (2.7 g, 13.4 mmol) in ether (200 mL) was added a hexane solution of butyllithium (1.6 M, 20 mL) at dry ice–acetone temperature under nitrogen. After being warmed to room temperature, the reaction mixture was quenched with D₂O (15 mL; Wako NMR solvent grade, D content >99%). After stirring for 1 h, the mixture was extracted with benzene. Evaporation of the solvent gave 2-(ethynyl-2-*d*)anthracene (2.6 g, 96%). No ¹H signal was detected at δ 3.20 in NMR spectra.

A THF solution of catecholborane²⁰ (Aldrich, 1.0 M, 15 mL, 15 mmol) was added to a refluxing THF solution (80 mL) of 2-(ethynyl-2-*d*)anthracene (2.6 g, 10.3 mmol). After 1 h an additional THF solution (15 mL) of catecholborane was added to the reaction mixture. After 6 h of refluxing, acetic acid (20 mL; Wako non-water titration grade) was added to the cooled reaction mixture. The mixture was refluxed overnight and extracted with benzene. Flash column chromatography (SiO₂, hexane) followed by crystallization of the crude product gave 2-(ethenyl-(*Z*)-2-*d*)anthracene (0.45 g, 17%). The D content was more than 99% as determined by GCMS (Shimadzu QP-2000) and NMR (JEOL JM-FX270 or Bruker MSL-400). ¹H NMR (CDCl₃) δ 5.36 (d, 1H, $J = 11$ Hz, Ar–C=CH), 6.93 (d, 1H, $J = 11$ Hz, Ar–CH=C), 7.37–7.58 (m, 3H, ArH), 7.69–8.08 (m, 4H, ArH), 8.37 (s, 2H, ArH); MS m/z 203 ((M – 2)⁺, 34.5%), 204 ((M – 1)⁺, 31.1%), 205 (M⁺, 100%) [cf. 2-EA: MS m/z 203 ((M – 1)⁺, 28.4%), 204 (M⁺, 100%), 205 ((M + 1)⁺, 16.4%)].

[†] Chiba University.

[‡] University of Tsukuba.

[§] Present address: Department of Mechanical Engineering, Faculty of Engineering, Tokushima University, Minamijosanjima-cho, Tokushima 770, Japan.

* Abstract published in *Advance ACS Abstracts*, December 15, 1993.

2-(Ethenyl-(E)-2-d)anthracene. 2-(Ethenyl-(E)-2-d)anthracene ((E)-2-EAD) was prepared from 2-ethynylantracene by hydroboration with catecholborane followed by deuteration with $\text{CD}_3\text{CO}_2\text{D}$.²⁰ The product was a 69:31 mixture of deuterated and undeuterated derivatives.¹⁷

1-(Ethenyl-(Z)-2-d)anthracene. 1-(Ethenyl-(Z)-2-d)anthracene was prepared from 1-ethynylantracene according to procedures similar to those employed for preparation of 2-(ethenyl-(Z)-2-d)anthracene; 1-ethynylantracene (10.6 g, 52 mmol) was brominated with bromine (8.3 g, 52 mmol) to give 1-(1,2-dibromoethyl)anthracene (16.8 g, 89%). The dibromide (16.8 g, 46 mmol) was dehydrobrominated with sodium amide to afford 1-ethynylantracene (2.1 g, 23%); $^1\text{H NMR}$ (CDCl_3) δ 3.58 (s, 1H, $\text{C}\equiv\text{CH}$), 7.34–8.40 (m, 7H, ArH), 8.54 (s, 1H, ArH), 9.40 (s, 1H, ArH). 1-Ethynylantracene (2.1 g, 10.4 mmol) was converted to 1-(ethynyl-2-d)anthracene (2.1 g, 99%) with butyllithium (1.6 M in hexane, 16 mL) and D_2O (15 mL). No ^1H signal was detected at δ 3.58 in NMR spectra.

1-(Ethenyl-2-d)anthracene (2.1 g, 8.3 mmol) was allowed to react with catecholborane (20 mmol) and quenched with acetic acid. Flash column chromatography (SiO_2 , hexane) and subsequent crystallization from petroleum ether of the crude product gave 1-(ethenyl-(Z)-2-d)anthracene (0.5 g, 24%, D content >98%); $^1\text{H NMR}$ (CDCl_3) δ 5.53 (d, 1H, $J = 11$ Hz, $\text{Ar}-\text{C}=\text{CH}$), 7.30–7.75 (m, 5H, $\text{Ar}-\text{CH}=\text{C}$ and ArH), 7.91–8.10 (m, 3H, ArH), 8.42 (s, 1H, ArH), 8.67 (s, 1H, ArH). MS m/z 203 ($(\text{M} - 2)^+$, 65.4%), 204 ($(\text{M} - 1)^+$, 100%), 205 (M^+ , 84.8%) [cf. 1-EA: MS m/z 203 ($(\text{M} - 1)^+$, 100%), 204 (M^+ , 85.6%), 205 ($(\text{M} + 1)^+$, 13.7%)].

9-(Ethenyl-(Z)-2-d)anthracene. 9-Anthraldehyde was allowed to react with the Wittig reagent prepared from (chloromethyl)triphenylphosphonium chloride²¹ (7.0 g, 20.1 mmol) and butyllithium (1.6 M in hexane, 18 mL) in THF. Column chromatography [SiO_2 , benzene:hexane (1:1)] of the crude product gave 9-(2-chloroethenyl)anthracene (2.1 g, 44%).

9-(2-Chloroethenyl)anthracene (1.5 g, 6.3 mmol) was treated with butyllithium (1.6 M in hexane, 5 mL) in ether at dry ice-acetone temperature, and the reaction mixture was quenched with D_2O (10 mL). After a quick workup, 1-(ethynyl-2-d)anthracene obtained (2.1 g, 8.3 mmol) was allowed to react with catecholborane (1.0 M in THF, 20 mL, 20 mmol) in THF and subsequently quenched with acetic acid (20 mL). Flash column chromatography (SiO_2 , hexane) followed by crystallization from petroleum ether of the crude product gave 9-(ethenyl-(Z)-2-d)anthracene (0.31 g, 24%, D content 93%); mp 166–167 °C; $^1\text{H NMR}$ (CDCl_3) δ 5.59 (d, 1H, $J = 15$ Hz, $\text{Ar}-\text{C}=\text{CH}$), 7.42–7.54 (m, 5H, $\text{Ar}-\text{CH}=\text{C}$ and ArH), 7.90–8.07 (m, 2H, ArH), 8.23–8.31 (m, 2H, ArH), 8.35 (s, 1H, ArH); MS m/z 203 ($(\text{M} - 2)^+$, 73.8%), 204 ($(\text{M} - 1)^+$, 100%), 205 (M^+ , 78.1%) [cf. 9-EA: MS m/z 203 ($(\text{M} - 1)^+$, 100%), 204 (M^+ , 83.1%), 205 ($(\text{M} + 1)^+$, 13.1%)].

Other Chemicals. Fluorenone and benzil were purified by crystallization from ethanol. Solvent benzene (Dotite Spectrozol) was used as received.

Absorption, Fluorescence, and Phosphorescence Spectra. Absorption spectra were measured on a JASCO UVIDEK-660 spectrophotometer. Fluorescence spectra were measured on a Hitachi F-4000 or F-4010 spectrofluorometer. Instrumental response was corrected by using rhodamine 6G. Phosphorescence spectra were also measured on a Hitachi F-4000 or F-4010 spectrofluorometer equipped with phosphorescence accessories.

Laser Flash Photolyses. An excimer laser (Lambda Physik EMG-101) was used as an excitation light source at 308 nm (XeCl, 10-ns fwhm) and also as a pumping light source (308 nm) of a dye laser (Lambda Physik FL3002) exciting at 425 nm (stilbene 3), with employing a computer-controlled system with a storage scope (Iwatsu TS-8123), as described in detail previously.²²

Measurements of Isomerization Quantum Yields. A degassed benzene solution of an (ethenyl-2-d)anthracene (EAD) and benzil

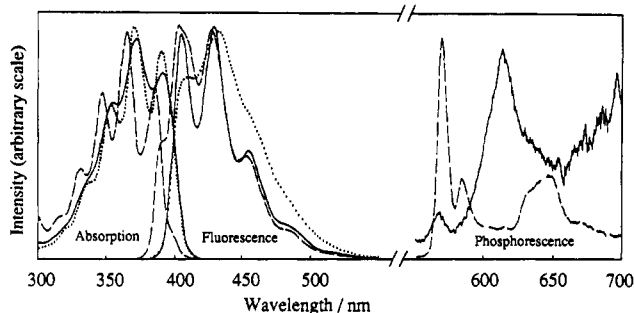


Figure 1. Absorption spectra (in benzene), fluorescence spectra (in argon-purged benzene) of 1-, 2-, and 9-EA (solid, dashed, and dotted line, respectively), and phosphorescence spectra of 1-EA (excitation at 372 nm; solid line) and 2-EA (excitation at 356 nm; dashed line) in degassed EPA at 77 K.

TABLE 1: Energetic and Kinetic Parameters of Ethenylantracenes

olefin	λ_f^a	E_S^b	λ_p^a	E_T^b	Φ_f	Φ_{isc}	$T_n \leftarrow T_1$ absorption		
							λ_{max}^c	ϵ_T^d	τ_T^e
2-EA	385	308	681	176	0.42	0.55	445	47700	101
1-EA	391	300	708	169	0.64	0.27	500	46600	64
9-EA	390	298	(725) ^f	165 ^f	0.91	0.05	415	20600	35

^a Wavelengths of the 0,0 bands of fluorescence (λ_f) and phosphorescence spectra (λ_p) in nm. ^b In kJ mol^{-1} . ^c In nanometers. ^d In $\text{cm}^{-1} \text{M}^{-1}$. ^e Triplet lifetimes in microseconds. ^f Determined from S-T absorption.

or fluorenone as a triplet sensitizer in a quartz cell was irradiated at varying temperatures in the cell room of a Hitachi F-4000 or F-4010 spectrofluorometer with an attached 150-W xenon lamp at 436 ± 10 nm. Light intensity was determined by potassium tris(oxalato)ferrate(III) actinometry,²³ and conversion of the olefin was determined by monitoring the signals of olefinic protons on a 60-MHz (Hitachi R-600), 270-MHz (JEOL JM-FX270), or 400-MHz (Bruker MSL 400) NMR spectrometer.

3. Results

3.1. Absorption, Fluorescence, and Phosphorescence Spectra.

Figure 1 depicts absorption (measured in benzene) and fluorescence spectra (measured in argon-purged benzene) of 1-, 2-, and 9-EA, and phosphorescence spectra (measured in deaerated EPA at 77 K) of 1- and 2-EA (no phosphorescence was observed for 9-EA). The maxima of their longest absorption bands are shifted to the longer wavelength in the order of 2-, 9-, and 1-EA. The absorption band exhibits a well-defined vibrational structure in 2-EA, but a less defined one in 1-EA and 9-EA.

The fluorescence quantum yields (Φ_f) were determined by comparison with anthracene as a standard ($\Phi_f = 0.27$)²⁴ and are included in Table 1. The singlet (E_S) and triplet excitation energies (E_T) determined from the 0,0 bands of the fluorescence and phosphorescence spectra are also listed in Table 1. The E_T value of 9-EA was determined as 165 kJ mol^{-1} from S-T absorption in CH_3I and CH_2Br_2 .

3.2. $T_n \leftarrow T_1$ Absorption. Laser flash photolyses of EAs (5×10^{-4} M) with 308-nm laser pulses in degassed benzene led to strong transient absorptions as shown in Figure 2. The transient absorption spectrum of 1-EA has an absorption maximum (λ_{max}) at 500 nm, and 2-EA has two maxima at 420 and 445 nm similar to those of anthracene. 9-EA has a broad absorption maximum around 415 nm. These transients are reasonably assigned to the $T_n \leftarrow T_1$ absorptions of EAs on the basis of similarity of the spectral profiles to those of the corresponding (E)-(3,3-dimethylbutenyl)anthracenes ((E)-DMBA).^{12,25} In addition, fluorenone (5×10^{-2} M) sensitization (excitation at 425 nm) of 1-, 2-, and 9-EA gave the same transient absorptions as observed on their direct excitation, respectively.

The lifetimes (τ_T) of these transients were determined in degassed benzene by monitoring the first-order decays at their

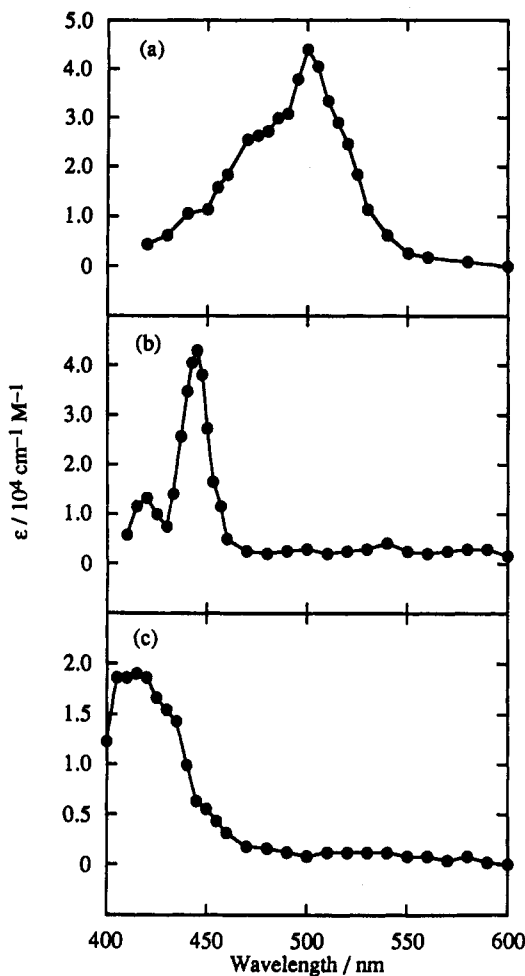


Figure 2. Transient absorption spectra obtained 3.0 μ s after laser excitation of 1-, 2-, and 9-EA (a, b, and c, respectively) in argon-purged benzene.

absorption maxima as 101, 64, and 35 μ s for 2-, 1-, and 9-EA, respectively, which were unvaried at temperatures between 7.1 and 43 $^{\circ}$ C within experimental uncertainty. 2-, 1-, and 9-EAD showed the same lifetimes as the corresponding EAs, respectively, therefore exhibiting no isotope effect. The τ_T values were larger in benzene degassed by freeze-thaw cycles than in the same solvent under argon bubbling.¹⁷ The above values are close to the triplet lifetimes (on the order of 10–100 μ s) of one-way isomerizing olefins such as 2-styrylanthracene.^{12,14}

For determination of molar extinction coefficients (ϵ_T) of $T_n \leftarrow T_1$ absorptions of ethenylanthracenes (EAs), a constant concentration (5×10^{-2} M) of fluorenone as triplet sensitizer was excited in benzene in the presence of varying concentrations of an EA ($(0.5\text{--}6) \times 10^{-2}$ M) or anthracene as a reference with a constant laser power (at 425 nm), and the resulting change of the absorbance (ΔA) at the absorption maximum was plotted against the concentration of EA. The ΔA value increased with increasing concentration of EA or anthracene, and attained a plateau region when the concentration was larger than ca. 0.02 M (more than 98% of the triplet sensitizer was quenched by EA or anthracene). Comparison of ΔA at the plateau region with that of anthracene ($\epsilon_T = 49\,800\text{ cm}^{-1}\text{ M}^{-1}$)²⁶ gave ϵ_T of EA. The ϵ_T values determined are 47 700, 46 600, and 20 600 $\text{cm}^{-1}\text{ M}^{-1}$ for 1-, 2-, and 9-EA, respectively.

The quantum yields for intersystem crossing (Φ_{isc}) of the isomeric EAs were determined by direct irradiation of optically matched (at 308 nm) benzene solutions of EAs and anthracene with a 308-nm laser and by comparison of ΔA s observed for EAs with that of anthracene ($\Phi_{isc} = 0.71$).²⁷ The determined Φ_{isc} values are 0.27, 0.55, and 0.05 for 1-, 2-, and 9-EA, respectively. The results are summarized in Table 1.

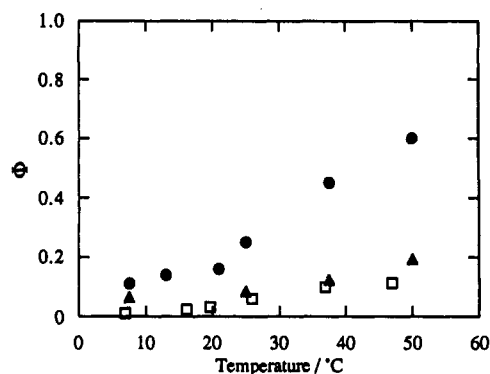


Figure 3. Plots of isomerization quantum yields of 1-EAD (1.5×10^{-2} M, solid circles), 2-EAD (1.0×10^{-2} M, open squares),¹⁷ and 9-EAD (1.5×10^{-2} M, solid triangles) against temperature.

TABLE 2: Quenching of EA Triplets by Some Typical Triplet Quenchers

quencher	E_S or E_T / kJ mol ⁻¹	$k_q/\text{M}^{-1}\text{ s}^{-1}$		
		1-EA	2-EA	9-EA
oxygen	94	2.8×10^9	3.1×10^9	2.2×10^9
perylene	147	7.5×10^9	7.8×10^9	6.7×10^9
azulene	167	1.1×10^9	5.3×10^9	8.7×10^7

To assign the conformation of T_1 species, either planar or twisted, the quenching rate constants (k_q) of $T_n \leftarrow T_1$ absorptions were measured for triplet quenchers such as oxygen ($E_S = 94$ kJ mol⁻¹),²⁸ perylene ($E_T = 147$ kJ mol⁻¹),²⁹ and azulene ($E_T = 167$ kJ mol⁻¹).²⁹ The obtained k_q values are listed in Table 2. The k_q values tend to decrease in the order of 2-, 1-, and 9-EA for every quencher examined. The k_q values of the three EAs for perylene are nearly diffusion controlled, and those for oxygen are in the same magnitude as reported for the quenching of the triplet state of rigid aromatic hydrocarbons such as anthracene.³⁰

3.3. Isomerization Quantum Yields. The quantum yields for isomerization of 1-, 2-, and 9-EAD (Φ) were measured at various temperatures. Conversion of the *Z* isomer to the *E* isomer was determined by integrating the signals of ethenyl β protons of EAD in the ¹H NMR spectrum. For (*Z*)-1-EAD (1.5×10^{-2} M), the samples were irradiated for 30 min by a 150-W xenon lamp at 436 ± 10 nm at temperatures between 6.2 and 50 $^{\circ}$ C in degassed benzene in the presence of fluorenone (1.5×10^{-2} M) as a triplet sensitizer. NMR spectra were measured after concentrating the reaction mixtures and replacing the solvent from benzene to benzene-*d*₆. The quantum yields determined are plotted as a function of the temperature in Figure 3.

To examine the effect of olefin concentration, the quantum yields were determined for (*Z*)-1-EAD in concentrations of 3.5×10^{-3} , 5.8×10^{-3} , and 8.9×10^{-3} M at ambient temperature; however, the quantum yield was practically constant in the above concentration range, as seen in the relative quantum yields of 1.00, 1.00, and 0.96 in that order of concentrations.

The quantum yields were also determined for (*Z*)-9-EAD (1.5×10^{-2} M) in the presence of fluorenone (1.5×10^{-2} M) at temperatures between 7.5 and 50 $^{\circ}$ C. For 2-EAD (1.0×10^{-2} M), *E* \rightarrow *Z* isomerization yields ($\Phi_{E \rightarrow Z}$) were previously determined¹⁷ on benzil (0.2 M)-sensitized irradiation (436 ± 10 nm) in degassed benzene at temperatures between 6.9 and 46.9 $^{\circ}$ C.

Experimental restrictions accompanied in accurate measurements of the quantum yields in low concentrations of (*Z*)- and (*E*)-EADs by NMR prevented us from examining the effect of the wide range of olefin concentration on the quantum yield, since a more accurate analytical method like HPLC used for DMBA could not be employed for the present purpose. Therefore, the quantum yields were determined at relatively high concentrations of the olefins, 3.5×10^{-3} – 1.5×10^{-2} M.

In Figure 3 also are plotted the determined quantum yields for 2- and 9-EAD against temperature. In all EADs, the isomer-

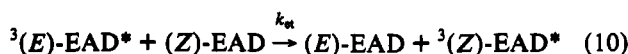
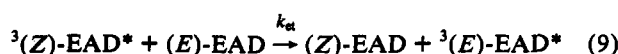
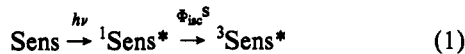
ization quantum yields tend to increase with temperature. The $\Phi_{E \rightarrow Z}$ values of 2-EAD and $\Phi_{Z \rightarrow E}$ of 9-EAD at ambient temperature are much smaller than those for styrenes¹⁻³ and stilbenes⁴ (≈ 0.5); however, $\Phi_{Z \rightarrow E}$ of 1-EAD are comparable with them. It is remarkable that $\Phi_{Z \rightarrow E}$ of 1-EAD at 50 °C is larger than 0.5, suggesting participation of a quantum chain process since the triplet potential energy surface is symmetrical about rotation of the olefinic bond (*vide infra*).

4. Discussion

$T_n \leftarrow T_1$ Absorption. The EA (or EAD) triplets have lifetimes of 30–100 μ s (Table 1), much longer than those of stilbenes⁷ and styrenes³¹⁻³³ (on the order of 10–100 ns); the triplet lifetimes are not affected by temperature. The EA triplets observed can be assigned to a planar geometry rather than a twisted one, since oxygen and perylene quench the EA triplets with rate constants of about 3×10^9 and 7×10^9 M⁻¹ s⁻¹, respectively (Table 2). If the EA triplets took a twisted geometry, they would be quenched by oxygen more rapidly through acceleration of intersystem crossing³⁴ but less efficiently by perylene because the twisted triplets of EAs are insufficient in energy to excite perylene.

These features indicate that the most stable triplet state takes an almost planar conformation rather than a twisted conformation; the planar conformation deactivates to the ground state very slowly with a 10–100- μ s lifetime.

Across-a-Ridge Isomerization on the Triplet Energy Surface. A striking feature of EAD isomerization on triplet sensitization is that the isomerization quantum yields depend upon temperature. This feature and temperature independence of the triplet lifetime imply that the isomerization between (E)-EAD and (Z)-EAD proceeds through an adiabatic conversion between $^3E^*$ and $^3Z^*$ on the triplet energy surface, and that the $^3p^*$ geometry is only a transition state of the conversion between $^3E^*$ and $^3Z^*$. In view of this mechanism, the relevant processes at the initial stage of sensitized reaction are expressed by eqs 1–10, where k_r means the



rate constant for double-bond rotation resulting in isomerization between triplet (E)-EAD and triplet (Z)-EAD, and k_d denotes the deactivation rate constant of triplet (E)-EAD and triplet (Z)-EAD. k_r and k_d are, respectively, supposed to be equal for the E and Z isomers of an olefin since the two isomers have essentially the same electronic structure. k_{et} is the rate constant for energy

transfer from triplet (E)-EAD to (Z)-EAD and from triplet (Z)-EAD to (E)-EAD.

At a low conversion of the Z to E isomer, $\Phi_{Z \rightarrow E}$ is expressed by the following equation based on the steady-state approximation for the above processes except eqs 4 and 9:

$$\Phi_{Z \rightarrow E} = \Phi_{isc}^S \Phi_{ET}^S \frac{k_r(k_d + k_{et}[(Z)\text{-EAD}])}{k_d(2k_r + k_d + k_{et}[(Z)\text{-EAD}])} \quad (11)$$

where Φ_{isc}^S and $\Phi_{ET}^S (=k_q[(Z)\text{-EAD}]/(k_d^S + k_q[(Z)\text{-EAD}]))$ represent the quantum yields for intersystem crossing of the excited singlet sensitizer and for energy transfer from the sensitizer triplet to the ground-state (Z)-EAD, respectively.

In the presence of a sufficient concentration of EAD, Φ_{ET}^S is reasonably assumed to be nearly unity, Φ_{isc}^S is nearly unity for the sensitizers used,³⁵ and therefore, $\Phi_{Z \rightarrow E}$ is expressed by eq 12:

$$\Phi_{Z \rightarrow E} = \frac{k_r}{k_d} \frac{k_d + k_{et}[(Z)\text{-EAD}]}{2k_r + k_d + k_{et}[(Z)\text{-EAD}]} \quad (12)$$

where the second fraction relates to the effect of concentration of the Z isomer on $\Phi_{Z \rightarrow E}$.

In the present series of EADs does the quantum chain process seem to participate since $\Phi_{Z \rightarrow E}$ for 1-EAD exceeds 0.5 in a relatively high concentration of 1.5×10^{-2} M at higher temperature. In an across-a-ridge isomerization on a symmetrical triplet energy surface about double-bond rotation, the ${}^3Z^* \rightarrow {}^3E^*$ conversion is followed by the ${}^3E^* \rightarrow {}^3Z^*$ reversion of the resulting ${}^3E^*$ with the same quantum yield as that of the forward process, and accordingly the quantum yield for $Z \rightarrow E$ isomerization is at most 0.5 when the quantum chain process is not involved. For EADs, however, contribution of the quantum chain process is much smaller than in the $Z \rightarrow E$ isomerization of DMBAs proceeding with quantum yields of 10–20 in the Z isomer concentrations on the order of 10^{-3} M.

From eq 12, k_r is given by the following equation:

$$k_r = \Phi_{Z \rightarrow E} k_d \frac{k_d + k_{et}[(Z)\text{-EAD}]}{k_d(1 - 2\Phi_{Z \rightarrow E}) + k_{et}[(Z)\text{-EAD}]} \quad (13)$$

However, in the infinitely dilute concentration of (Z)-EAD, the second fraction of eq 12 is $k_d/(2k_r + k_d)$, and therefore $\Phi_{Z \rightarrow E} = k_r/(2k_r + k_d)$. In a sufficiently high concentration of (Z)-EAD and also under the present experimental condition, the second fraction of eq 12 is unity, and therefore $\Phi_{Z \rightarrow E} \approx k_r/k_d$. At these concentrations, $k_r \approx \Phi_{Z \rightarrow E} k_d$.

The k_r values estimated by using eq 13 with $k_{et} = 1 \times 10^8$ M⁻¹ s⁻¹, the corresponding k_{et} value for the one-way isomerizing 2-anthrylethylenes,^{12,14} are listed in Table 3 together with the k_d values determined. The estimated k_r values are essentially unaffected by the k_{et} values in the range of 10^8 – 10^9 M⁻¹ s⁻¹. Figure 4 depicts the Arrhenius plots of k_r and k_d . The k_d value is essentially unvaried with temperature examined, and the k_r value is increased with temperature. The activation energies and the preexponential factors obtained are included in Table 3 along with the activation enthalpy, entropy, and free energy (ΔH^* , ΔS^* , and ΔG^* , respectively).

The k_r values increase in the order of 2-, 1-, and 9-EAD, and the values for E_a , A , ΔH^* , and ΔS^* decrease in that order. This sequence of ΔH^* values for isomerization must reflect the increasing extent of the interaction between the ethenyl and anthryl groups in the above order as seen in the orbital coefficients of LUMO of the ethenyl carbons and ipso carbon of the anthracene nucleus.³⁶ The negative ΔS^* values indicate a more ordered character of the transition state for isomerization than the planar conformation. In the isomerization of 9-EA, the rotation of double bond releases steric hindrance around the single bond between the ethenyl and aromatic groups and achieves conjugation of the π lobes of the α -carbon with those of the aromatic group. The ΔS^* and ΔH^* values compensate each other to give nearly the

TABLE 3: Kinetic Parameters for Adiabatic Isomerization of the Triplet State of EAD

olefin	k_T/s^{-1} ^a	k_d/s^{-1} ^b	k_T/k_d ^a	E_a ^c	A/s^{-1}	ΔH^\ddagger ^{c,d}	ΔS^\ddagger ^{d,e}	ΔG^\ddagger ^{c,d}
2-EAD	1.1×10^3 ^f	1.0×10^4	0.11	46	5.0×10^{10}	42	-40	54
1-EAD	9.5×10^3	1.6×10^4	0.59	32	1.6×10^9	30	-67	50
9-EAD	5.5×10^3	2.8×10^4	0.19	19	6.3×10^6	17	-113	50

^a At 323 K. ^b Mean values of those observed at various temperatures. ^c In kJ mol⁻¹. ^d At 300 K. ^e In J K⁻¹ mol⁻¹. ^f Estimated from the Arrhenius equation.

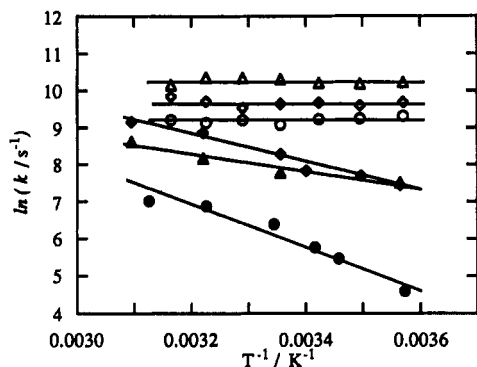


Figure 4. Arrhenius plots for the C=C bond rotation on the triplet energy surface (k_T : solid marks) and for deactivation from the triplet excited state (k_d : open marks) for 1-, 2-, and 9-EAD (squares, circles, and triangles, respectively).

same value of ΔG^\ddagger , 50–54 kJ mol⁻¹, independent of the substitution position of the ethenyl group on the anthracene nucleus. Therefore, these values are governed by the steric and electronic effect of the substitution position.

Triplet Potential Energy Surface. On the assumption that ³EAD* and ³EA* possess the same energy surface, we can depict the triplet energy surface against the angle of rotation about the ethylenic bond, i.e., the isomerization coordinate. The planar geometry of 2-EAD triplets is by 176 kJ mol⁻¹ above the ground state as evaluated from the phosphorescence data. Since this value is very close to the triplet energies of anthracene (179 kJ mol⁻¹) and (*E*)-DMBA (178 kJ mol⁻¹), the phosphorescent state of 2-EAD can be ascribed to the planar geometry. The triplet energies of the planar conformation of 1-EA and 9-EA are estimated as 169 and 165 kJ mol⁻¹ from the phosphorescence and S-T absorption, respectively. The magnitude of k_q for azulene also suggests that the energies of the lowest triplet of EAs are in the vicinity of that of azulene.²⁵ The triplet energies of twisted geometry (³p*) are estimated on the basis of the activation energy for isomerization.

The triplet energy surfaces of EA and EAD are completely different from those of styrenes¹⁻³ and stilbenes.⁴ A plausible explanation is that avoided crossings between an "ethylenic" triplet state (ψ_a) with an energy minimum at the twisted geometry and "aromatic" triplet states (ψ_b) with an energy minimum at the planar geometry retain a shallow energy minimum, if any, at the twisted geometry of the lowest triplet state. This situation may be accomplished by a high extent of the stabilization of ψ_a by substitution of an anthracene group carrying a low triplet energy on the ethylenic carbon.^{32,37} A very short residence time at ³p* in EAD results in a rapid rotation to the planar triplet conformation rather than inefficient deactivation from ³p* to the ground state.³⁵ Stabilization of the triplet state at ³E* and even at ³p* in the order of 9-, 1-, and 2-EA must be explained as the extent of interaction of the ethenyl and anthryl groups as discussed above.

The present results for 1-, 2-, and 9-EAD provide further evidence for the presence of considerable activation barriers in the triplet state of one-way isomerizing olefins as previously shown for 1-, 2-, and 9-DMBA, of which the ³Z* → ³E* isomerization requires the energy barriers of 13–25 kJ mol⁻¹.²⁵

Acknowledgment. We thank the Ministry of Education, Science and Culture for the partial support of this work by Grants-in-Aid for Specially Promoted Research No. 03101004 (K.T., T.A., T.K.,

and H.S.) and for Scientific Research Nos. 02453019 (K.T.) and 01740255 (T.A.) and also thank The University of Tsukuba for the President's Special Grant for Education and Research (K.T.). We thank Professor Yoshihisa Inoue, Himeji Institute of Technology, for his valuable discussion and to Professor Noritake Kusumi (presently Tokushima University), Professor Naomichi Furukawa, and Dr. Tatsuya Nabeshima (presently Gunma University), University of Tsukuba, for their kind arrangements for the use of their analytical facilities.

References and Notes

- (1) Caldwell, R. A.; Sovocool, G. W.; Peresie, R. J. *J. Am. Chem. Soc.* **1973**, *95*, 1496.
- (2) Bonneau, R. *J. Photochem.* **1979**, *10*, 439.
- (3) Arai, T.; Sakuragi, H.; Tokumaru, K. *Bull. Chem. Soc. Jpn.* **1982**, *55*, 2204.
- (4) Saltiel, J.; Charlton, J. L. In *Rearrangement in Ground and Excited States*; de Mayo, P., Ed.; Academic Press: New York, 1980; Vol. 3, p 25.
- (5) Saltiel, J.; Marchand, G. R.; Kirkor-Kaminska, E.; Smothers, W. K.; Mueller, W. B.; Charlton, J. L. *J. Am. Chem. Soc.* **1984**, *106*, 3144.
- (6) Saltiel, J.; Rousseau, A. D.; Thomas, B. *J. Am. Chem. Soc.* **1983**, *105*, 7631.
- (7) Görner, H.; Schulte-Frohlinde, D. *J. Phys. Chem.* **1981**, *85*, 1835.
- (8) Schulte-Frohlinde, D.; Görner, H. *Pure Appl. Chem.* **1979**, *51*, 279.
- (9) Görner, H.; Schulte-Frohlinde, D. *J. Photochem.* **1978**, *8*, 91.
- (10) Gegiou, D.; Muszkat, K. A.; Fischer, E. *J. Am. Chem. Soc.* **1968**, *90*, 3907.
- (11) Arai, T.; Karatsu, T.; Sakuragi, H.; Tokumaru, K. *Tetrahedron Lett.* **1983**, *24*, 2873.
- (12) Karatsu, T.; Arai, T.; Sakuragi, H.; Tokumaru, K. *Chem. Phys. Lett.* **1985**, *115*, 9.
- (13) Hamaguchi, H.; Tasumi, M.; Karatsu, T.; Arai, T.; Tokumaru, K. *J. Am. Chem. Soc.* **1986**, *108*, 1698.
- (14) (a) Arai, T.; Karatsu, T.; Misawa, H.; Kuriyama, Y.; Okamoto, H.; Hiresaki, T.; Furuuchi, H.; Zeng, H.; Sakuragi, H.; Tokumaru, K. *Pure Appl. Chem.* **1988**, *60*, 989. (b) Tokumaru, K.; Arai, T. *J. Photochem. Photobiol. A: Chem.* **1992**, *65*, 1. (c) Arai, T.; Tokumaru, K. *Chem. Rev.* **1993**, *93*, 23.
- (15) Bartocci, G.; Maesetti, F.; Mazzucato, U.; Spalletti, A.; Orlandi, G.; Poggi, G. *J. Chem. Soc., Faraday Trans. 2* **1988**, *84*, 385.
- (16) Karatsu, T.; Tsuchiya, M.; Arai, T.; Sakuragi, H.; Tokumaru, K. *Chem. Phys. Lett.* **1990**, *169*, 36.
- (17) Misawa, H.; Karatsu, T.; Arai, T.; Sakuragi, H.; Tokumaru, K. *Chem. Phys. Lett.* **1988**, *146*, 405.
- (18) Stolka, M.; Yanus, J. F.; Pearson, J. M. *Macromolecules* **1976**, *9*, 710. Stolka, M.; Yanus, J. F.; Pearson, J. M. *Ibid.* **1976**, *9*, 715.
- (19) Campbell, K. N.; Campbell, B. K. *Organic Syntheses*; Wiley: New York, 1963; Collect. Vol. IV, p 763.
- (20) Brown, H. C.; Gupta, S. K. *J. Am. Chem. Soc.* **1975**, *97*, 5249.
- (21) Köbrich, G.; Trapp, H.; Flory, K.; Drischel, W. *Chem. Ber.* **1966**, *99*, 689.
- (22) Karatsu, T.; Hiresaki, T.; Arai, T.; Sakuragi, H.; Tokumaru, K. *Bull. Chem. Soc. Jpn.* **1992**, *64*, 3355.
- (23) Murov, S. L. *Handbook of Photochemistry*; Dekker: New York, 1973; p 119.
- (24) Melhuish, W. H. *J. Phys. Chem.* **1961**, *65*, 229.
- (25) Karatsu, T.; Kitamura, A.; Zeng, H.; Arai, T.; Sakuragi, H.; Tokumaru, K. *Chem. Phys. Lett.* **1992**, *2193*.
- (26) Carmichael, I.; Helman, W. P.; Hug, G. L. *J. Phys. Chem. Ref. Data* **1987**, *16*, 239.
- (27) Amand, B.; Bensasson, R. *Chem. Phys. Lett.* **1975**, *34*, 44.
- (28) Reference 23, p 5.
- (29) Gijzeman, O. L. J.; Kauffman, F.; Porter, G. *J. Chem. Soc., Faraday Trans. 2* **1973**, *69*, 708.
- (30) (a) Gorman, A. A.; Hamblett, I.; Harrison, R. J. *J. Am. Chem. Soc.* **1984**, *106*, 6952. (b) Merkel, P. B.; Kearns, D. *J. Chem. Phys.* **1973**, *58*, 398.
- (31) Bonneau, R. *J. Am. Chem. Soc.* **1980**, *102*, 3816.
- (32) Caldwell, R. A.; Pac, C. *Chem. Phys. Lett.* **1979**, *64*, 303.
- (33) Caldwell, R. A.; Cao, C. V. *J. Am. Chem. Soc.* **1981**, *103*, 3594.
- (34) Arai, T.; Karatsu, T.; Sakuragi, H.; Tokumaru, K. *Chem. Lett.* **1981**, 1377.
- (35) Reference 23, p 50.
- (36) Calculations were made by a PPP-SCF-CI method. The coefficients of LUMO for ipso-, α -, and β -carbons are 0.25, 0.09, 0.21 for 2-EA, 0.31, 0.11, 0.27 for 1-EA, and 0.40, 0.14, 0.34 for 9-EA, respectively. Further studies with AM1 and MNDO calculations are in progress.
- (37) Kikuchi, O.; Segawa, K.; Takahashi, O.; Arai, T.; Tokumaru, K. *Bull. Chem. Soc. Jpn.* **1992**, *65*, 1463.